

Journal Pre-proof

Cardiac protection induced by urocortin-2 enables the regulation of apoptosis and fibrosis after ischemia and reperfusion involving miR-29a modulation

Isabel Mayoral-González, Eva M. Calderón-Sánchez, Isabel Galeano-Otero, Marta Martín-Bórnez, Encarnación Gutiérrez-Carretero, María Fernández-Velasco, Nieves Domenech, María Generosa Crespo-Leiro, Ana María Gómez, Antonio Ordóñez-Fernández, Abdelkrim Hmadcha, Tarik Smani

PII: S2162-2531(22)00008-7

DOI: <https://doi.org/10.1016/j.omtn.2022.01.003>

Reference: OMTN 1489

To appear in: *Molecular Therapy: Nucleic Acid*

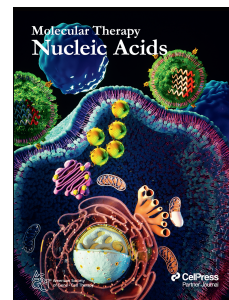
Received Date: 11 May 2021

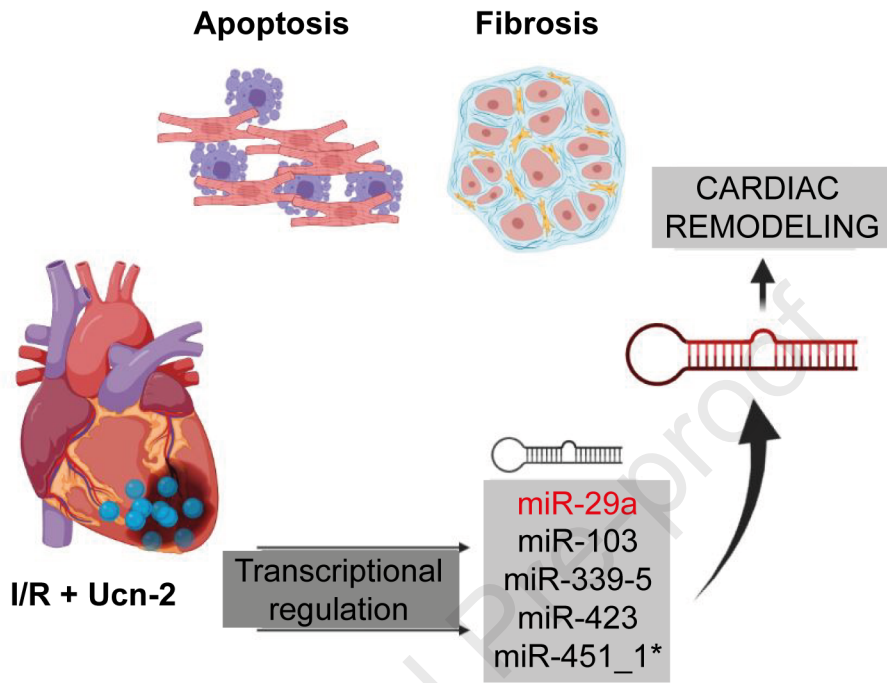
Accepted Date: 7 January 2022

Please cite this article as: Mayoral-González I, Calderón-Sánchez EM, Galeano-Otero I, Martín-Bórnez M, Gutiérrez-Carretero E, Fernández-Velasco M, Domenech N, Crespo-Leiro MG, Gómez AM, Ordóñez-Fernández A, Hmadcha A, Smani T, Cardiac protection induced by urocortin-2 enables the regulation of apoptosis and fibrosis after ischemia and reperfusion involving miR-29a modulation, *Molecular Therapy: Nucleic Acid* (2022), doi: <https://doi.org/10.1016/j.omtn.2022.01.003>.

This is a PDF file of an article that has undergone enhancements after acceptance, such as the addition of a cover page and metadata, and formatting for readability, but it is not yet the definitive version of record. This version will undergo additional copyediting, typesetting and review before it is published in its final form, but we are providing this version to give early visibility of the article. Please note that, during the production process, errors may be discovered which could affect the content, and all legal disclaimers that apply to the journal pertain.

© 2022





1 **Cardiac protection induced by urocortin-2 enables the regulation of apoptosis**
2 **and fibrosis after ischemia and reperfusion involving miR-29a modulation**

3

4 **Isabel Mayoral-González^{1,2}, Eva M. Calderón-Sánchez^{2,3,&}, Isabel Galeano-**
5 **Otero^{2,4,&}, Marta Martín-Bórniz^{1,2}, Encarnación Gutiérrez-Carretero^{1,2,3}, María**
6 **Fernández-Velasco^{3,5}, Nieves Domenech^{3,6}, María Generosa Crespo-Leiro^{3,6},**
7 **Ana María Gómez⁷, Antonio Ordóñez-Fernández^{1,2,3}, Abdelkrim Hmadcha^{8,9,*},**
8 **Tarik Smani^{2,3,4*}.**

9 ¹Department of Surgery, University of Seville, Seville, Spain.

10 ²Group of Cardiovascular Pathophysiology, Institute of Biomedicine of Seville,
11 University Hospital of Virgen del Rocío/University of Seville/CSIC, Seville,
12 Spain.

13 ³Centro de Investigación Biomédica en Red Enfermedades Cardiovasculares.
14 (CIBERCV), Madrid, Spain

15 ⁴Department of Medical Physiology and Biophysics, University of Seville, Seville,
16 Spain.

17 ⁵Innate Immune Response Group, IdiPAZ, La Paz University Hospital, Madrid,
18 Spain.

19 ⁶Cardiology Department, Instituto de Investigación Biomédica de A Coruña,
20 Complejo Hospitalario Universitario de A Coruña, Servicio Gallego de Salud,
21 Universidade da Coruña, Coruña, Spain.

22 ⁷Signaling and Cardiovascular Pathophysiology, INSERM, Université Paris
23 Saclay, 92296 Châtenay-Malabry, France.

24 ⁸Department of Biotechnology, University of Alicante, Alicante. University of
25 Pablo Olavide, Sevilla.

26 ⁹Spanish Biomedical Research Centre in Diabetes and Associated Metabolic
27 Disorders (CIBERDEM), Madrid, Spain.

28 [&]These authors contribute equally to this manuscript

29

30 *Correspondence should be addressed to T.S. (tasmani@us.es) and A.H.
31 (khmadcha@upo.es).

32 Instituto de Biomedicina de Sevilla (IBiS), Hospital Universitario Virgen del
33 Rocío. Avenida Manuel Siurot S/N, Sevilla 41013, Spain.

34 Phone: (+34) 955 92 30 57; Fax: (+34) 955 92 31 01.

35

36 **Short title:** Ucn-2 implicates miR-29a regulation in heart infarction

37 **ABSTRACT**

38 Urocortin-2 (Ucn-2) has demonstrated cardioprotective actions against
39 myocardial ischemia-reperfusion (I/R) injuries. Herein, we explored the
40 protective role of Ucn-2 through microRNAs (miRNAs) post-transcriptional
41 regulation of apoptotic and pro-fibrotic genes. We determined that the
42 intravenous administration of Ucn-2 before heart's reperfusion in Wistar rat
43 model of I/R recovered cardiac contractility and reduced fibrosis, LDH release,
44 and apoptosis. The infusion of Ucn-2 also inhibited the upregulation of 6
45 miRNAs in revascularized heart. The *in silico* analysis indicated that miR-29a and
46 miR-451_1* are predicted to target many apoptotic and fibrotic genes.
47 Accordingly, the transfection of neonatal rat ventricular myocytes with mimics
48 overexpressing miR-29a, but not miR-451_1*, prevented I/R-induced expression
49 of pro- and anti-apoptotic genes such as *Apaf-1*, *Hmox-1* and *Cyts*; as well as pro-
50 fibrotic genes *Col-I* and *Col-III*. We also confirmed that *Hmox-1*, target of miR-
51 29a, is highly expressed at mRNA and protein level in adult rat heart under I/R;
52 whereas, Ucn-2 abolished I/R induced mRNA and protein upregulation of
53 HMOX-1. Interestingly, a significant upregulation of *Hmox-1* was observed in the
54 ventricle of ischemic patients with heart failure, correlating negatively with the
55 left ventricle ejection fraction. Altogether, these data indicate that Ucn-2 through
56 miR-29a regulation, provides long-lasting cardioprotection, involving post-
57 transcriptional regulation of apoptotic and fibrotic genes.

58

59 **Abbreviations:**

60 AIFM-1, apoptosis-inducing factor 1, mitochondrial; AMI, acute myocardial
61 infarction; APAF-1, apoptosis protease-activating factor-1; BCL-2, B-Cell
62 lymphoma 2;; COL-I, collagen-I; COL-III, collagen-III; CYCS, cytochrome C; CRF-
63 R2, corticotropin releasing factor receptor 2; HF, heart failure; HMOX-1, heme
64 oxygenase 1; I/R, ischemia and reperfusion; LVEF, Left Ventricle Ejection
65 Fraction; MAPK-8, mitogen-activated protein kinase 8; miRNAs, microRNAs;
66 NVRMs, neonatal ventricle rat myocytes; pPCI, primary percutaneous coronary
67 intervention; TGF- β , transforming growth factor β ; Ucn-2, Urocortin-2.

68

69

70

71

72

73

74

75

76 **INTRODUCTION**

77 Acute myocardial infarction (AMI) is one of the major causes of morbidity
78 and mortality worldwide.¹ AMI sequelae, such as apoptosis of cardiac myocytes
79 in the so-called border or risk zone near the infarct scars are known to trigger the
80 adverse cardiac remodeling and aggravate cardiac dysfunction.^{2,3} Benefits of
81 timely and effective early revascularization after AMI are well-recognized.
82 However, the process of myocardial revascularization is associated with critical
83 injuries that occur when oxygen rich blood re-enter the vulnerable myocardial
84 tissue, a phenomenon known as ischemia and reperfusion (I/R) syndrome.⁴
85 Lethal complications of I/R injuries cause the adverse cardiac remodeling and
86 consequently heart failure.^{5,6} Therefore, effective strategies in cardioprotection
87 are still eagerly needed.

88 In recent years, evidences demonstrated that urocortin 2 (Ucn-2) has
89 cardioprotective effects on myocardial I/R injuries and heart failure.⁷ Ucn-2 is an
90 endogenous peptide belonging to the corticotropin releasing factor (CRF) family.
91 Ucn-2 binds with high affinity to the receptor CRF-R2 that is highly expressed in
92 the cardiovascular system.⁸ The administration of Ucn-2 evokes important
93 changes in the cardiovascular system, such as human coronary vasodilatation,⁹
94 and triggers potent cardioprotective effects against I/R injuries since it decreases
95 the infarct size and prevents harmful cell death.¹⁰ Similarly, the other isoform
96 Ucn-1 induces positive inotropic and lusitropic effects in rats,¹¹ improves the
97 intracellular calcium concentration ($[Ca^{2+}]_i$) handling in I/R,¹² and efficiently

98 protects hearts from I/R injuries by the modulation of apoptotic genes, such as
99 *Cd40lg*, *Xiap* and *Bad*.¹³ The infusion of Ucn-2 into the rat I/R-model also promotes
100 cardioprotection, involving changes in the expression of microRNAs (miRNAs),
101 which play major role in the post-transcriptional regulation of genes.¹⁴ MiRNAs
102 are small non-coding RNAs that regulate a plethora of cellular processes related
103 to AMI, including cardiac myocyte apoptosis, necrosis and fibrosis.¹⁵ They play
104 critical roles in heart function under pathophysiological conditions and also in
105 different cardioprotection strategies.^{16,17} Recently, we demonstrated that the
106 levels of different miRNAs changed rapidly into the bloodstream of patients
107 suffering from AMI with ST-segment elevation (STEMI) undergoing primary
108 percutaneous coronary intervention (pPCI), and were related to the development
109 of the adverse cardiac remodeling.¹⁸

110 In the present study, we evaluated the role of Ucn-2 in the regulation of
111 miRNAs expression under I/R, focusing on a list of circulating miRNAs whose
112 levels changed in infarcted patients after pPCI. We further examined the role of
113 miRNAs in the regulation of pro-fibrotic and apoptotic genes induced by I/R.

114 **RESULTS**

115 **I/R increases circulating Ucn-2 and the expression of CRF-R2 in heart's tissue**

116 Since Ucn-2 is an endogenous stress-related peptide, we examined its
117 concentration in serum of I/R rat model following the experimental protocol
118 illustrated in Supplemental Figure 1A. Figure 1A shows that the concentration of
119 Ucn-2 increased significantly 1 week after heart's intervention, as compared to

120 sham, meanwhile it decreased 6 weeks after surgery. We also assessed the
121 expression of Ucn-2 receptor (CRF-R2) in risk zone of the infarcted heart. Figure
122 1B shows that the expression of CRF-R2 was significantly increased 1 week after
123 I/R, comparing to sham. In contrast, the expression of CRF-R2 was restored 6
124 weeks after surgery. Therefore, the level of circulating Ucn-2 and the expression
125 of CRF-R2 increased transiently after the heart infarction and its
126 revascularization.

127 **Ucn-2 recovers heart contractility and prevents I/R-induced fibrosis**

128 We investigated the cardioprotective effect of Ucn-2 (150 µg/Kg) infused 5
129 min before reperfusion, using different approaches. Data in Figure 2A and Table
130 1 indicate that 1 week after surgery the left ventricle ejection fraction (LVEF), the
131 fractional shortening (LVFS), as well as the left ventricular end-diastolic volume
132 (LVEDV) and the left ventricular end-systolic volume (LVEsV), recovered
133 significantly in Ucn-2 treated rats, as compared to I/R non-treated rats.
134 Meanwhile, I/R induced increase in the left ventricle diastolic diameter (LVdD)
135 was not affected by Ucn-2. Next, we examined the effect of Ucn-2 on cardiac
136 fibrosis. As shown in Figure 2B-D the administration of Ucn-2 decreased the
137 fibrotic areas of the infarcted hearts assessed *in vivo* by cardiac magnetic
138 resonance and by Masson's trichrome staining. Moreover, Figure 2E-H shows
139 that the expression of pro-fibrotic genes *Collagen-I (Col-I)*, *Collagen-III (Col-III)*,
140 *Transforming Growth Factor β -1 (Tgf- β 1)* and *Transforming Growth Factor β -2 (Tgf-*
141 *β 2)* increased significantly in the risk zone of hearts isolated 1 week after I/R. By

142 contrast, rats treated with Ucn-2 showed significantly reduced expression of
143 these pro-fibrotic genes.

144 **Ucn-2 prevents I/R-induced apoptosis**

145 To further evaluate the cardioprotection exerted by Ucn-2, we examined its
146 action on cardiac myocytes viability and death. As illustrated in Figure 3A the
147 administration of Ucn-2 decreased significantly I/R-evoked lactate
148 dehydrogenase (LDH) concentrations, increased 24 h after I/R. Following the
149 experiment protocol outlined in Supplemental Figure 1A, Figure 3B shows that
150 Ucn-2 infusion in I/R rat markedly reduced the number of apoptotic cardiac
151 myocytes, as assessed by TUNEL assay. Ucn-2 treatment also trended to decrease
152 I/R-evoked caspase 3 cleavage (Figure 3C). To confirm these results, we examined
153 Ucn-2 effect on adult rat ventricle myocytes (ARVM), using annexin V staining.
154 As depicted in Figure 3D-F, Ucn-2 pre-treatment of cardiac myocytes exposed to
155 I/R decreased the number of apoptotic cells stained by annexin V, while it
156 preserved the number of living cells. Altogether, these data indicate that the
157 infusion of Ucn-2 at the onset of reperfusion preserves cardiac cell viability and
158 attenuates apoptosis.

159 **Ucn-2 modulates the expression of miRNAs in the heart under I/R**

160 Given the importance of the post-transcriptional regulation of the expression
161 of genes in cardiac pathophysiological processes,^{14,19} we examined whether Ucn-
162 2 could regulate the expression of miRNAs in hearts excised from I/R rats model.
163 We selected a list of miRNAs based on the analysis of circulating miRNAs

164 released in patients with STEMI who underwent revascularization with primary
165 Percutaneous Coronary Intervention (pPCI), as described recently,¹⁸ since little is
166 known about the role of those miRNAs in I/R and whether they can be good
167 target for cardioprotective drugs. Figure 4A shows a list of circulating miRNAs
168 released in serum of STEMI patients 3 h after the angioplasty. The expression of
169 miR-29a, miR-103, miR-125a-3p, miR-133, miR-139-3p, miR-320, miR-324-3p,
170 miR-324-5p, miR-339-5p, miR-423_1, miR-451_1* and miR-499-5p were also
171 detected in heart samples isolated from atrium biopsies of ischemic patients with
172 heart failure (HF) (Figure 4B). Based on these findings, we examined the
173 expression of these 12 human miRNAs in I/R rats' ventricle isolated from the risk
174 area. As illustrated in Figure 4C-H, the expression of miR-29a, miR-103, miR-133,
175 miR-339-5p, miR-423_1 and miR-451_1* was significantly upregulated at 24 h
176 and 1 week after I/R, except for miR-133 that showed a downregulation at 1 week
177 after I/R. In contrast, the administration of Ucn-2 5 min before heart's
178 revascularization prevented significantly I/R-induced upregulation of these
179 miRNAs, excluding miR-423_1 which was not sensitive to Ucn-2 24 h after I/R.
180 Supplemental Figure 2 shows that I/R evoked significant increase in the
181 expression of miR-125a, miR-139, miR-320, and miR-324-3p at 24 h, but not of
182 miR-324-5p and miR-499_1, while the administration of Ucn-2 did not prevent
183 the overexpression of these miRNAs. Therefore, Ucn-2 efficiently modulated the
184 expression of some miRNAs associated with pPCI in STEMI patients, which are
185 altered by I/R in heart tissue of rats.

186 **miR-29a and miR-451_1* are predicted to modulate the expression of genes**
187 **related to apoptosis and cell survival pathway**

188 To determine target genes of miR-29a, miR-103, miR-133, miR-339-5p, miR-
189 423_1 and miR-451_1*, we performed an *in silico* analysis using PANTHER
190 software. As illustrated in Figure 5A the analysis generated a pie chart suggesting
191 that miRNAs have predicted target genes are involved in pathways of apoptosis
192 and fibrosis. Specifically, 41 signaling pathways are mainly implicated in cellular
193 processes associated with post-AMI, such as apoptosis and fibrosis. Interestingly,
194 we found that only miR-29a and miR-451_1* are predicted to target 16 and 17
195 apoptotic genes, and 14 and 18 genes related to fibrosis, respectively (Figure 5B).

196 Based on this analysis and to assess the role of miR-29a and miR-451_1* in the
197 regulation of those predicted genes we performed the quantitative RT PrimePCR
198 array, using the Bio-Rad predesigned assay specifically for apoptosis and
199 survival pathway (Supplemental Figure 3A). Experiments were performed in
200 neonatal rat ventricular myocytes (NRVM) transfected with mimics of miRNAs
201 to overexpress miR-29a and miR-451_1*, under *in vitro* I/R protocol as explained
202 in Supplemental Figure 1B. First, we checked if the expression of miR-29a and
203 miR-451_1* are similarly sensitive to I/R in NRVM and adult heart. Accordantly,
204 Supplemental Figure 3B and C confirms that I/R enhanced the expression of miR-
205 29a and miR-451_1*, while Ucn-2 significantly inhibited both miRNAs in a
206 similar way in NRVM and in adult rat heart. Second, Supplemental Figure 3D

207 and E shows that NRVM transfection with mimics of miR-29a and miR-451_1*
208 successfully increased the levels of miR-29a and miR-451-1*.

209 Figure 5C and Supplemental table 1 show that 56 genes were upregulated and
210 20 downregulated 24 h after I/R in NRVM. By contrast, in NRVM transfected with
211 mimics of miR-29a and miR-451_1*, 56 and 49 genes were downregulated, while
212 20 and 27 genes were upregulated, respectively (Figure 5D and 5E; Supplemental
213 table 1). These data indicate that mimics of miR-29a and miR-451_1* reverted the
214 expression of many apoptotic genes overexpressed under I/R.

215 **miR-29a regulates the expression of I/R-induced apoptotic and fibrotic genes**

216 To verify the results of the PrimePCR array we examined the expression of 6
217 selected genes in NRVM transfected with mimics of miR-29a and miR-451_1*
218 under I/R. The selection of these genes was based on their fold change rates as
219 well as their implication in I/R-related processes, as published elsewhere.²⁰⁻²²
220 Namely, we investigated the expression of *Apoptosis Inducing Factor mitochondria*
221 *associated 1 (Aifm1)*, *Apoptosis Protease-Activating Factor-1 (Apaf1)*, *B-Cell Lymphoma*
222 *2 (Bcl-2)*, *Cytochrome C (Cycs)*, *Heme Oxygenase 1 (Hmox-1)* and *Mitogen-Activated*
223 *Protein Kinase 8 (Mapk-8)*. Figure 6A and B shows that the expression of *Apaf-1*
224 and *Hmox-1* increased significantly in I/R, as compared to control. Figure 6C
225 indicates that the expression of *Cycs* slightly increased under I/R, although not
226 significantly. However, the expression of *Aifm-1*, *Bcl-2* and *Mapk-8* was not
227 affected by I/R, as compared to control (Figure 6D, E and F). Conversely, mimic
228 of miR-29a, but not of miR-451_1*, prevented I/R effects on *Apaf-1*, *Hmox-1*, and

229 *Cyts* (Figure 6A-C). Meanwhile, miR-29a enhanced the expression of *Aifm-1*
230 (Figure 6D), and decreased the expression of *Mapk-8* (Figure 6F) under I/R. In
231 contrast, miR-451_1* mimic significantly increased the expression of *Hmox-1* and
232 *Mapk-8*, comparing to their levels in I/R (Figure 6C and F). The expression of *Bcl-*
233 *2* was not affected either by I/R or miRNAs mimics. Moreover, we analyzed if
234 miR-29a and miR-451_1* could target pro-fibrotic genes in NRVM, as is the case
235 of the effect of Ucn-2 in tissue of adult heart shown previously in Figure 2. Figure
236 6G and H shows that I/R induced small but significant upregulation of *Col-I* and
237 *Col-III*, which was significantly downregulated by miR-29a. Of note, miR-451_1*
238 also failed to modulate the expression of *Col-I* and *Col-III*. These data indicate that
239 miR-29a, but not miR-451-1*, modulated I/R-induced overexpression of *Apaf-1*,
240 *Hmox-1*, *Cyts*, *Col-I* and *Col-III*.

241 **Signaling pathway involved in miR-29a regulation by Ucn-2**

242 Once we determined that miR-29a efficiently modulated I/R-induced changes
243 in the expression of apoptotic and fibrotic genes, we studied the signaling
244 pathway involved in the regulation of miR-29a by Ucn-2 applied in NRVM under
245 I/R (Supplemental Figure 1C). Figure 6I shows that NRVM treatment with Ucn-
246 2 (10 nM) before reperfusion inhibited I/R-induced miR-29a overexpression,
247 whereas NRVM pretreatment with astressin (0.5 μ M), the specific antagonist of
248 CRF-R2 receptor,²³ significantly attenuated Ucn-2 effect. CRF-R2 is known to
249 couple Gs/cAMP/PKA signalling, therefore we investigated if Ucn-2 action was
250 mediated by of PKA or Epac (exchange protein directly activated by cAMP). Our

251 data show that NRVM pretreatment with ESI-05 (10 μ M), specific inhibitor of
252 Epac2,²⁴ abolished Ucn-2 downregulation of miR-29a. By contrast, PKA
253 inhibition with H89 (1 μ M) did not significantly affect Ucn-2 downregulation of
254 miR-29a. Finally, because Epac activates the Ras1-ERK1/2 pathway,²⁶ we
255 examined whether ERK1/2 participates in Ucn-2 action. Nevertheless, the
256 inhibition of ERK1/2 by PD 098059 (5 μ M)²⁸ did not inhibit significantly Ucn-2-
257 effect on miR-29a under I/R. Altogether, these data demonstrate that the
258 administration of Ucn-2 before reperfusion modulated the expression miR-29a
259 through the activation of CRF-R2 and Epac2.

260 **I/R induced changes in the expression of apoptotic genes in rat's ventricle**

261 To confirm if these genes are relevant in the adult infarcted heart, we
262 examined their expression in I/R rats infused with Ucn-2. Figure 7A-C shows that
263 mRNA expression of *Hmox-1*, *Aifm-1* and *Apaf-1* were increased in risk zones 24
264 h after I/R, but it significantly decreased 1 week after the intervention. Moreover,
265 the administration of Ucn-2 blocked I/R-evoked *Hmox-1* upregulation, while it
266 enhanced I/R-induced expression of *Aifm-1*. In contrast, Figure 7D shows that
267 mRNA expression of *Cyts* significantly decreased 24 h, but it recovered after 1
268 week after I/R. The expression of *Cyts* as well as *Apaf-1* was not affected by Ucn-
269 2 (Figure 7C, D). At the same time, we did not observe significant changes in the
270 expression of *Mapk-8* under any experimental conditions, while Ucn-2 induced
271 *Bcl-2* increase 24 h after I/R (Supplemental Figure 4). Interestingly, as shown in
272 Figure 7E and F the protein expression of HMOX-1 and AIFM-1 were

273 significantly increased in risk zone of I/R rats 24 h after surgery, but Ucn-2
274 potently reduced HMOX-1 expression and tended to decrease the upregulation
275 of AIFM-1. By contrast, CYCS protein was not affected by I/R nor by Ucn-2
276 (Figure 7G).

277 Finally, we assessed the expression of these genes in ventricle biopsies of
278 patients with HF of ischemic origin. Figure 8A shows that only the expression of
279 *Hmox-1* was significantly increased, as compared to a healthy ventricle sample.
280 The expression of *Apaf-1* and *Aifm-1* slightly but not significantly trend to
281 increase in those patients. Meanwhile, the expression of *Mapk-8* and *Cycs* tended
282 to decrease in these samples. Interestingly, the analysis of a possible correlation
283 between patients' LVEF and these genes expression shows significant negative
284 correlations between the expression of *Hmox-1*, *Mapk-8*, and *Cycs* with the LVEF
285 of the patients, whereas the expression of *Apaf-1* and *Aifm-1* did not correlate with
286 the LVEF (Figure 8B-F). Altogether, these results suggest that HF patients might
287 overexpress genes related to apoptosis in function of the severity of their HF,
288 although higher number of samples is necessary to confirm this preliminary
289 observation.

290 **DISCUSSION**

291 Despite the overwhelming advances in cardiovascular therapies HF
292 following AMI remains the leading cause of mortality and morbidity in humans.
293 Therefore, strategies of cardioprotection are of major interest to limit I/R injuries
294 and cardiac myocytes loss after AMI.²⁵ This study confirms the important

295 protective role of the administration of Ucn-2 at early reperfusion which
296 mitigates I/R injuries. We observed significant and transient increase in
297 circulating Ucn-2 and the expression of its receptor CRF-R2, 1 week after I/R. This
298 result agree with previous studies which proposed Ucn-2 as a potential
299 diagnostic and prognostic biomarker for cardiovascular diseases.^{27,29} Ucn-2
300 belongs to the stress hormone CRF family; therefore, our data confirm that under
301 the stress caused by I/R, the heart enhances not only the circulating Ucn-2 but
302 also its CRF-R2 receptor to activate the related signaling pathway in the injured
303 heart. Moreover, we demonstrate that intravenous infusion of Ucn-2 improves
304 cardiac contractility after I/R since it increases LVEsV and decreases the LVEdV,
305 indicating successful heart contraction and relaxation. In addition, using
306 different approaches we demonstrate that Ucn-2 decreases significantly I/R-
307 induced fibrosis, which will preserve myocardial compliance and will prevent
308 impaired cardiac diastolic and systolic function evoked by I/R.

309 I/R-induced cardiac cells death in affected hearts is another important factor
310 contributing to cardiac dysfunction and cardiac remodelling. Here, we
311 demonstrate that Ucn-2 reduces LDH amount, and we observe less cleaved
312 caspase 3 staining and DNA fragmentation, indicative of apoptosis, in Ucn-2
313 infused I/R rats. Annexin V staining further confirms that Ucn-2 prevents ARVM
314 death and increase cell survival, in accordance with our previously published
315 data.^{10,14}

316 One of the limitations of the infusion of cardioprotective drugs is related to
317 their limited benefits duration due to their short half-life. Recent studies
318 indicated that Ucn-2 gene transfer provides sustained increase in the
319 concentration of plasma Ucn-2 and enhanced cardiac function in normal mice
320 and in mice with HF,^{30,31} although its role in modulating I/R stress was not
321 assessed. Herein, we provide evidences demonstrating that Ucn-2 modulates
322 changes in miRNAs, post-transcriptional gene expression, and protein
323 expression, in agreement with previous studies.^{14,32} We decided to study the
324 effect of Ucn-2 on miRNAs which have been recently detected in blood samples
325 of STEMI patients undergoing pPCI,¹⁸ and in failing heart samples, because little
326 is known about the role of those human miRNAs in cardiac function after I/R.
327 Our results using adult rats and isolated cardiac myocytes unveil the ability of
328 Ucn-2 to modulate the expression of 6 of those miRNAs that are rapidly released
329 to the blood stream after pPCI in STEMI patients. In fact, we demonstrate that
330 Ucn-2 infusion prevents I/R-evoked upregulation of miR-29a, miR-103, miR-133,
331 miR-339-5p, miR-423_1 and miR-451_1, in rats. This effect was even sustained 1
332 week after heart reperfusion, indicating at least a medium lasting action of Ucn-
333 2 on miRNAs dysregulation.

334 Based on the *in silico* and PrimePCR findings, we found that miR-29a and
335 miR-451_1* possibly target many genes associated with apoptosis and fibrosis,
336 two prevalent pathways during the early adverse cardiac remodeling. We
337 demonstrate that the overexpression of miR-29a, but not miR-451_1*, efficiently

338 prevent the expression of collagen mRNA, indicating fibrosis inhibition in
339 agreement with recent studies which showed that miR-29a inhibits fibrosis in
340 myocardial infarcted rats,³³ in heart stressed with isoproterenol by
341 downregulating the expression of *DNA Methyltransferase enzymes A (Dnmt3a)*,³⁴
342 and in heart derived from chemotherapy.³⁵ Furthermore, miR-29a overexpression
343 prevents I/R-induced upregulation of *Apaf-1*, *Cyts*, and *Hmox-1*; meanwhile it
344 increases the expression of *Aifm-1*. As known, the intrinsic mitochondrial
345 apoptotic pathway is initiated after reperfusion by the release of *Cyts* into the
346 cytoplasm which stimulates *Apaf-1* and procaspase-9 in the apoptosome,
347 inducing apoptosis.³⁶⁻³⁸ Thus, *Apaf-1*, *Aifm-1* and *Cyts* are considered pro-
348 apoptotic genes. By contrast, *Hmox-1* is considered anti-apoptotic and
349 cardioprotective. For instance, its gene delivery prevents cardiac remodeling and
350 preserves cardiac function after myocardial infarction, as described previously.³⁹
351 Other studies demonstrated that the transplantation of mesenchymal stem cells
352 overexpressing *Hmox-1* conferred cardioprotection against ischemic injury in
353 heart and skeletal muscle.^{40,41} There is a general consensus that cardiac myocyte
354 activates both pro- and anti-apoptotic pathways during the progressive
355 transition of the heart from a situation of adaptation to one of maladjustment
356 after I/R.⁴² Therefore, miR-29a and its predicted target genes could be a potential
357 regulator of a balance between pro- and anti-apoptotic processes. miR-29a has
358 been reported to play other beneficial role in cardiovascular homeostasis, such as

359 cardiac hypertrophy,⁴³ and modulation of cardiac cell metabolism,⁴⁴ indicating
360 their potential features as therapeutic agent.

361 In this study, we also show in adult rat heart that HMOX-1 can be regulated
362 by Ucn-2, in the same way as miR-29a, both at mRNA and protein levels. By
363 contrast, Ucn-2 modulates differentially AIFM-1 at mRNA and protein levels,
364 indicating that perhaps Ucn-2 affects the post-translational process of some
365 protein. This finding suggest that the protective effect of Ucn-2 does not occur
366 exclusively through miR-29a and may involve other mediators that could act
367 differentially in post-transcriptional and post-translational processes.
368 Interestingly, we demonstrate that Ucn-2 regulates the expression of miR-29a
369 through the activation of CRF-R2 and Epac2, which is consistent with the role of
370 Epac2 on miR-139-3p and miR-324 modulation by Ucn-1 isoform in cardiac
371 myocytes.¹⁴

372 Furthermore, we provide preliminary data showing that ischemic patients
373 with HF overexpress *Hmox-1*, while the expression of other apoptotic genes seem
374 not significantly altered. We demonstrate a negative correlation between LVEF
375 of HF patient and the expression of *Hmox-1*, *Cyts* and *Mapk-8*, which may be
376 related to the *Cyts*-mediated cell death pathway. Although, the overexpression
377 of *Hmox-1* was unexpected since this gene is sought to exert anti-inflammatory
378 and anti-apoptotic effects post-AMI.⁴⁵ Perhaps, the overexpression of *Hmox-1*
379 may play a role in sustaining and protecting the still non-affected tissue of the

380 infarcted heart in those HF patients when their LVEF is severely compromised.

381 Further experiments are needed to clarify these data.

382 To summarize, this study demonstrate that Ucn-2 provides long-lasting
383 cardioprotective effects involving miRNAs regulation, which target apoptosis
384 and fibrosis. Mimicking changes of the expression of miRNAs caused by Ucn-2,
385 combined with functional studies, allows us to efficiently identify new role of
386 miR-29a in myocardial I/R, that presumably leads to a balanced regulation of
387 anti- and pro-apoptotic pathways.

388

389 **MATERIALS AND METHODS**

390 This study was performed in accordance with the recommendations of the Royal
391 Decree 53/2013 in agreement to the Directive 2010/63/EU of the European
392 Parliament and approved by the local Ethics Committee on Human and animal
393 Research of A Coruña and University Hospital of Virgen del Rocio of Seville.

394 **Blood human samples and myocardial biopsies from patients with heart** 395 **failure**

396 Human serum was obtained from blood samples from patients who suffered a
397 first STEMI by centrifugation at 1500 g for 15 min, as detailed in previously.¹⁸ The
398 inclusion criteria were patients under 75 years old, diagnosed with AMI,
399 presenting symptoms 2 to 6 h prior to angioplasty and exhibiting epicardial TIMI
400 (Thrombolysis in Myocardial Infarction) flow grade of 0 in the initial angiogram.
401 Patients with a previous history of ischemic heart disease, a glomerular filtration

402 rate less than 30 mL/min, TIMI flow grade > 1 at the time of angiography were
403 excluded. Patients received standard pharmacological therapy as per current
404 clinical guidelines.

405 Myocardial biopsies were obtained from the atrium of 5 males and 2 females with
406 a median age of 62 years, and LVEF = $52.8 \pm 2.1\%$, before surgery. Left ventricle
407 biopsies of ischemic patients with HF were obtained from 4 males and 3 females,
408 with a median age of 58.6 years and LVEF = $31.7 \pm 6.4\%$. We also used one
409 ventricle biopsy from a healthy donor. These samples were obtained from
410 patients during surgery for cardiac transplantation at the University Hospital of
411 Virgen del Rocio in Seville and in A Coruña Hospital. A signed informed written
412 consent was provided from the families of all donors.

413 **Rat model of myocardial Ischemia and Reperfusion (I/R)**

414 The I/R rat model was performed using male Wistar rats weighing 250 ± 50 g as
415 previously described.¹⁰ Briefly, rats were anesthetized with intraperitoneal (i.p.)
416 injection of 50 mg/Kg ketamine plus 8 mg/Kg xylazine and were maintained with
417 a mixture of 2% O₂/sevoflurane during the whole procedure. A left thoracotomy
418 was performed in the intercostal space followed by a pericardiotomy. To induce
419 the stenosis a 6/0 Prolene™ (Ethicon™, NJ, US) nylon suture was placed around
420 the left anterior descendent coronary artery, reducing the vascular light using a
421 small piece of PE-10 tube that was placed-in-between for a convenient release
422 upon reperfusion. Analgesia was provided during the 3 days following surgery.

423 **In vivo experimental groups**

424 As shown in Supplemental Figure 1A, experimental group in rat model were
425 divided in: "Sham" group: rats undergoing the same surgical procedure without
426 coronary ligation. "I/R" group: ischemia was produced by ligation of the left
427 coronary artery during 40 min, afterward 0.9% NaCl solution was added through
428 tail veins 5 min before reperfusion. "I/R + Ucn-2" group: Same as I/R group but
429 i.v. dose of Ucn-2 (150 µg/Kg) was administered 5 min before reperfusion.
430 Experiments were performed especially in risk zone of the infarcted heart, which
431 belongs to the adjacent areas of the artery ligation.^{10,46} Three end points (24 h, 1
432 week and 6 weeks) were used depending on the experiment.

433 **Adult rat ventricle myocytes (ARVMs) primary culture**

434 The hearts were removed and mounted on a Langendorff perfusion apparatus.
435 Adult rat ventricle myocytes (ARVM) were isolated using collagenase type II (251
436 IU/mL) (Worthington Biochemical, CA, US) as described previously R.¹² Isolated
437 cells were filtered, centrifuged, and suspended in Tyrode solution containing
438 (mM): 130 NaCl, 1 CaCl₂, 0.5 MgCl₂, 5.4 KCl, 22 glucose, 25 HEPES, 0.4
439 NaH₂PO₄, 5 NaHCO₃) (pH 7.4). ARVM were plated in control solution
440 containing 1.8 mM CaCl₂ at 37°C and were later subjected to a protocol of I/R as
441 summarized in Supplemental Figure 1B, using a simulated ischemic solution
442 (mM): 142 NaCl, 3.6 KCl, 1.2 MgCl₂, 1.8 CaCl₂, 5 NaHCO₃, 20 HEPES, 20 Lactate-
443 Na, 20 sucrose (pH 6.22), as described previously.^{14,47} Cells were placed during 30
444 min in an incubator at 1% O₂ and 5% CO₂. Afterward, cells were reoxygenated
445 in control solution and maintained in at 21% O₂ and 5% CO₂ for 18-24 h. 30 nM

446 Ucn-2 was added before reperfusion. All experiments were performed on Ca²⁺-
447 tolerant rod-shaped myocytes.

448 **Neonatal Rat Ventricle Myocytes (NRVMs) primary culture**

449 Neonatal Rat Ventricle Cardiac myocytes (NRVMs) were isolated from the heart
450 of 1-3 days old Wistar rats. The primary ventricular cardiac myocytes were
451 cultured in Dulbecco's Modified Eagle Medium (DMEM)/medium 199 (4:1)
452 supplemented with 10% horse serum, 15% fetal bovine serum (FBS), 1%
453 glutamine, 100 U/ml penicillin and 100 µg/ml streptomycin for 24 h, later the
454 medium was replaced.

455 For miRNAs experiments, NRVMs were transfected at 70% of confluence, 48 h
456 after isolation, according to the manufacturer's instructions, using Lipofectamine
457 RNAiMAX Transfection Reagent (Thermo Fisher Scientific, US) with 10 µM of
458 mimics Rno -miR 29a (5' UAGCACCAUCUGAAAUCGGUUA 3'), Rno -miR 451
459 (5'AAACCGUUACCAUUACUGAGUU 3') or negative-control (Ambion,
460 Thermo Fisher, MA, US). 24 h later cells were exposed to the protocol of I/R as
461 illustrated in the Supplemental Figure 1B.

462 For pharmacological study, NRVM were incubated with inhibitors 10 min before
463 their exposition to I/R ± Ucn-2 (Supplemental Figure 1C).

464 **Echocardiography and Cardiovascular Magnetic Resonance**

465 Transthoracic echocardiographic and the cardiac magnetic resonance analysis
466 were performed as described previously¹⁰. The cardiac function was assessed 1
467 week after surgery in light anesthetized rats with 2% sevoflurane by Vevo™ 2100

468 ultrasound system with a transducer MS250 using a frequency range of 13-24
469 MHz (VisualSonics™, Toronto, Canada). M-Mode images of the left ventricle at
470 the level of the papillary muscles were obtained, and functional hemodynamic
471 parameters were recorded as the left ventricle ejection fraction (LVEF), left
472 ventricle ejection fraction; (LVFS), left ventricle end diastolic diameter (LVE_dD),
473 left ventricle end-diastolic Volume (LVE_dV), and left ventricle end-systolic
474 Volume (LVE_sV).

475 The cardiac magnetic resonance study was performed with the imaging system
476 ICON 1T (Bruker, Rheinstetten, Germany) using a rat whole body coil. To
477 quantify the ischemic area, images were collected with gradient echo T1
478 sequences and synchronized with the electrocardiogram (repetition time: 100 ms,
479 echo time: 2.5 ms, resolution: 0.234 × 0.234 mm, slice thickness: 1.250 mm, angle
480 of rotation: 75° or 90°, 2 cuts with the same geometry as the previous film
481 sequences, 15 min after the introduction of a gadolinium-based contrast to
482 highlight fibrotic areas. The acquisition of images and their analysis were
483 performed in a blind manner.

484 **Masson's trichrome staining**

485 Hearts from the three experimental groups were fixed with formalin and
486 embedded in paraffin. Hearts were cut into 6 μm sections and Masson's
487 trichrome protocol was performed to determine fibrosis stained in blue. Tissue
488 without fibrosis was stained in red.

489 **Tunnel assay and cleaved caspase 3 immunofluorescence.**

490 Hearts of rats were dissected, washed in cold PBS for blood clearance, and fixed
491 with 4% paraphormaldehyde. Sections were immersed in OCT and frozen to -
492 80°C and later cut in 6 μ M slices. For Tunnel assay, heart sections were stained
493 using the in-situ Cell Death Detection Kit, with fluorescein (Roche, Basel,
494 Switzerland) following the instruction of the manufacturer. Tunnel-positive
495 nuclei fluoresced bright green at 480–500 nm. Images were taken by widefield
496 Thunder microscope Leica (Leica, Westzlar, Germany) with computational
497 clearance at 10X.

498 For Caspase 3 immunofluorescence, heart sections were incubated overnight
499 with primary anti-cleaved Caspase 3 antibody (Cell Signalling, MA, US). After
500 washing, sections were incubated with a secondary antibody Alexa Fluor 594
501 (Thermo Fisher Scientific, MA, US). Wheat germ agglutinin (WGA) conjugated
502 with Alexa-fluor 488 was used to stain cell membrane, while DAPI was used to
503 stain nuclei. Five snapshots per condition were acquired using a fluorescence
504 microscope Olympus BX61 (Tokio, Japan) with 40X objective, and images were
505 analyzed to count the different proportion of red stained cells with ImageJ 1.45
506 software (Wayne Rasband, National Institute of Health, Bethesda, MD, USA).

507 **Annexin V-FITC staining**

508 Annexin V-FITC staining was used to detect apoptosis in adult rat cardiac
509 myocytes seeded in 6-channel μ -Slides VI 0,4 (Ibidi, Gräfelfing, Germany),
510 incubated with 100 μ l of the binding buffer supplied with the kit (Trevigen, MN,
511 US), and 1 μ l of annexin-FITC reagent, during 35 min at 25°C. Images were taken

512 with confocal microscope Leica TCS SP2 (Leica, Westzlar, Germany). Five
513 snapshots per condition were acquired using a HCX PI Apo CS dry 20X objective
514 with 2x zoom in z-stacks intervals, and maximum projection was recorded and
515 analyzed with Image J software ImageJ 1.45 software (Wayne Rasband, National
516 Institute of Health, Bethesda, MD USA), to count the proportion of labeled cells.
517 All assays were performed per triplicate, and counts were independently
518 conducted by two people in a blind manner.

519 **Elisa**

520 Serum of rats from the 3 experimental groups were purified using separation
521 columns. The level of Ucn-2 was determined by immunofluorescence assay
522 (Phoenix Pharmaceuticals, CA, US) following manufacturer instructions. The
523 level of LDH was detected by LDH-Glo™ Cytotoxicity Assay (Promega, WI, US).

524 **RNA extraction and qRT-PCR analysis**

525 miRNeasy Serum/Plasma kit (Qiagen, Hilden, Germany) was used to extract
526 small RNAs from patient's serum following the manufacturer instructions.
527 Taqman® array miRNAs cards pool A (Applied Biosystem, CA, US) was also
528 used to determine changes in the expression of miRNA using Viiia7 Real-Time
529 PCR system (Applied Biosystems, CA, US). The plate design includes
530 mammalian U6, RNU44 and RNU46 as endogenous control.
531 For tissue samples, miRNeasy kit (Qiagen, Hilden, Germany) was used to extract
532 total RNA or miRNAs following manufacturer instructions. Samples were
533 quantified using Nanodrop (Thermo Fisher Scientific, MA, US) for RNA and by

534 Qubit™ (Thermo Fisher Scientific, MA, US) for miRNAs. Reverse transcription
535 reactions were performed using miScript II RT Kit (Qiagen, Germany) (500 ng),
536 in accordance with the manufacturer's protocols. Prior to qRT-PCR reactions,
537 cDNA was diluted 1 in 5 for PCR assays.

538 PCR assays of miRNAs were performed using 10X universal primer (miScript
539 SYBR Green PCR Kit, Qiagen, Hilden, Germany), Sybr Green reactive (iTaq™
540 Universal SYBR Green Supermix, Bio-Rad, CA, US), and specific oligos of each
541 miRNA: miR-103, miR-125a, miR-133, miR-139, miR-29a, miR-320, miR-324-3p,
542 miR-324-5p, miR-339-5p, miR-423_1, miR-451_1* and miR-499_1 (Qiagen,
543 Hilden, Germany) according to the manufacturer instructions, using a ViiA 7
544 Real-Time PCR System (Applied Biosystems, MA, US). The average expression
545 levels of miRNAs in cells were normalized to miRTC1.

546 Reactions for genes PCR assays were performed in a 10 μ L reaction mixture
547 volume with 100 nM forward primer and 100 nM reverse primer for mRNA.
548 Primer sequences are described in Supplemental Table 2. The average expression
549 levels of genes were normalized to β -actin.

550 ViiA 7 Software version 1.2 (Life Technologies, Carlsbad, CA, USA) was used to
551 calculate the quantification cycle (Ct) value, which is defined as the number of
552 cycles at which the fluorescence signal is significantly above the threshold;
553 expression of each mRNA and miRNA was defined from the threshold cycle (Ct),
554 and relative expression levels were calculated using the $2^{-\Delta\Delta Ct}$ method after
555 normalization with the internal control, miRTC1 and β -actin for miRNA and

556 mRNA, respectively. Data are expressed as relative expression of Log Fold
557 change of means \pm Standard Error of the Mean (\pm SEM) of at least 4 replicates of
558 each experiment.

559 **PrimePCR assay**

560 We used PrimePCR (Bio-Rad, CA, US) predesigned assay (Apoptosis and
561 Survival Tier 1 H96), containing primers of validated genes specifically for
562 apoptosis and survival pathway, as indicated in Supplemental table 1 and figure
563 2. A mix of 4 samples were added and the reaction was performed according to
564 the manufacturer's instructions, on a Viia7 Real-Time PCR system (Applied
565 Biosystems, CA, US). The average expression levels of genes were normalized to
566 the expression of housekeeping gene HPRT1.

567 **In silico analysis of targeted genes by miRNAs**

568 The analysis of targeted genes predicted to be regulated by miRNAs was done
569 using different bioinformatics resources: miRBD (miRDB v7.2, <http://mirdb.org>,
570 Washington University St. Louis, MO, US) ,TargetScan (Release 7.1,
571 www.targetscan.org, Cambridge, MA, US) databases, and Exiqon tool
572 application (<http://www.exiqon.com/microna-target-prediction>). To identify
573 miRNA target gene pathways, we also used the online platform Gene Ontology
574 (GO) browser PANTHER (Protein Analysis THrough Evolutionary
575 Relationships) v14.1, (<http://pantherdb.org/genelistanalysis.do>, University of
576 Southern California, Los Angeles, CA, US).

577 **Western Blotting**

578 Protein extraction was carried out using NP40 Cell Lysis Buffer (Thermo Fisher
579 Scientific, MA, US) and quantified by Bradford method. Rat heart tissue was pre-
580 lysed using TissueLyser II (Qiagen, Hilden, Germany) before protein lysis buffer
581 addition. Protein samples were subjected to SDS-PAGE (10% acrylamide) and
582 electrotransferred onto PVDF membranes. After blocking with 5% non-fat dry
583 milk dissolved in Tris-buffered saline containing 0.1% Tween-20 (TTBS) for 1 h
584 at 37°C, membranes were probed overnight at 4°C with anti-CRF-R2 (Novus, CO,
585 US), anti-tubulin (Merck-Sigma-Aldrich, MI, US), anti-HMOX1 (Cell Signaling,
586 MA, US), anti-AIFM1 (Cell Signaling, MA, US) and anti-GAPDH (Sigma-Aldrich,
587 MI, US), in TTBS with 1% of BSA. After washing, membranes were incubated for
588 45 min at room temperature with a horseradish peroxidase conjugated with anti-
589 IgG (Cell Signaling, MA, US). Detection was performed in the ImageQuant LAS
590 4000 mini (GE Healthcare, IL, US). Images were analyzed with ImageJ software.

591 **Statistical analysis**

592 Analyzes were performed with GraphPad (GraphPad Software, Inc., CA, US),
593 using Shapiro-Wilk as normality test. For normally distributed variables we used
594 the Ordinary one-way ANOVA, and we performed the multiples comparisons
595 using *t* test without correction (Fisher's LSD test). We also used the non-
596 parametric test Kruskal-Wallis with multiple comparisons corrected by Dunn's
597 Test for non-normally distributed variables. Values were subjected to Log-
598 transformation to represent numerical features in the dataset to have a mean of 0
599 and a variance of 1 and to express data as "Relative gene/miR expression (Log

600 Fold Change)”. The outliers were removed based on results of QuickCalcs, an
601 online tool of Graphpad. Results are presented as the mean \pm SEM.

602

603 **AUTHOR CONTRIBUTIONS**

604 Conceptualization, A.H., and T.S.; funding acquisition, A.H., A.O., E.C.-S, and
605 T.S.; investigation, I.M.-G., E.C.-S., I.G.-O, E.G.-C, A.O., and T.S.; methodology,
606 I.M.-G., E.C.-S., I.G.-O, M.M.B., N.D., A.G., M.F.-V., A.H., and T.S.; project
607 administration, A.O., T.S.; writing—original draft, I.M.-G. and T.S.; and
608 writing—review and editing, N.D., M.C.-L, M.F.-V., A.G., D.-R.A., A.O., A.H.,
609 and T.S.

610

611 **CONFLICT OF INTEREST**

612 The authors declare that the research was conducted in the absence of any
613 commercial or financial relationships that could be interpreted as a potential
614 conflict of interest.

615

616 **FUNDING**

617 This study was co-financed by FEDER Funds [US-1381135], Agencia Estatal de
618 Investigación [PID2019-104084GB-C22/AEI/10.13039/501100011033]; the Institute
619 of Carlos III [PI18/01197; Red TerCel-Grant RD16/0011/0034]; the Andalusia
620 Government [grant number: PI-0193-2018]; and by Agence National de la
621 Recherche [ANR-19-14-0031-01].

622

623 **ACKNOWLEDGEMENTS**

624 We wish to thank Eva Sanchez de Rojas de Pedro for her technical help. Graphical
625 abstract was created with Biorender.com (<http://biorender.io>).

626

627 **Keywords:** Ischemia and Reperfusion, miRNA, heart failure, apoptosis, fibrosis,
628 Ucn-2, cardiac remodeling.

629

630 **REFERENCES**

- 631 1. Bahit, M.C., Kochar, A., and Granger, C.B. (2018). Post-Myocardial
632 Infarction Heart Failure. *JACC Hear. Fail.* 6, 179–186.
- 633 2. Abbate, A., and Narula, J. (2012). Role of Apoptosis in Adverse
634 Ventricular Remodeling. *Heart Fail. Clin.* 8, 79–86.
- 635 3. Feuerstein, G.Z. (2001). Apoptosis - New opportunities for novel
636 therapeutics for heart diseases. In *Cardiovascular Drugs and Therapy*
637 (Cardiovasc Drugs Ther), pp. 547–551.
- 638 4. Yellon, D.M., and Hausenloy, D.J. (2007). Myocardial Reperfusion Injury.
639 *N Engl J Med* 357, 1121–35.
- 640 5. Eltzschig, H.K., and Eckle, T. (2011). Ischemia and reperfusion-from
641 mechanism to translation. *Nat Med* 17.
- 642 6. González-Montero, J., Brito, R., Gajardo, A.I., and Rodrigo, R. (2018).
643 Myocardial reperfusion injury and oxidative stress: Therapeutic

- 644 opportunities. *World J. Cardiol.* 10, 74–86.
- 645 7. Monteiro-Pinto, C., Adão, R., Leite-Moreira, A.F., and Brás-Silva, C.
646 (2019). Cardiovascular Effects of Urocortin-2: Pathophysiological
647 Mechanisms and Therapeutic Potential. *Cardiovasc. Drugs Ther.* 33, 599–
648 613.
- 649 8. Van Pett, K., Viau, V., Bittencourt, J.C., Chan, R.K.W., Li, H.Y., Arias, C.,
650 Prins, G.S., Perrin, M., Vale, W., and Sawchenko, P.E. (2000). Distribution
651 of mRNAs encoding CRF receptors in brain and pituitary of rat and
652 mouse. *J. Comp. Neurol.* 428, 191–212.
- 653 9. Smani, T., Calderon, E., Rodriguez-Moyano, M., Dominguez-Rodriguez,
654 A., Diaz, I., and Ordóñez, A. (2011). Urocortin-2 induces vasorelaxation of
655 coronary arteries isolated from patients with heart failure. *Clin. Exp.*
656 *Pharmacol. Physiol.* 38, 71–76.
- 657 10. Domínguez-Rodríguez, A., Mayoral-Gonzalez, I., Avila-Medina, J., de
658 Rojas-de Pedro, E.S., Calderón-Sánchez, E., Díaz, I., Hmadcha, A.,
659 Castellano, A., Rosado, J.A., Benitah, J.-P., et al. (2018). Urocortin-2
660 Prevents Dysregulation of Ca²⁺ Homeostasis and Improves Early Cardiac
661 Remodeling After Ischemia and Reperfusion. *Front. Physiol.* 9, 813.
- 662 11. Calderón-Sanchez, E., Delgado, C., Ruiz-Hurtado, G., Domínguez-
663 Rodríguez, A., Cachafeiro, V., Rodríguez-Moyano, M., Gomez, A.M.,
664 Ordóñez, A., and Smani, T. (2009). Urocortin induces positive inotropic
665 effect in rat heart. *Cardiovasc. Res.* 83, 717–25.

- 666 12. Calderón-Sánchez, E.M., Ruiz-Hurtado, G., Smani, T., Delgado, C.,
667 Benitah, J.P., Gómez, A.M., and Ordóñez, A. (2011). Cardioprotective
668 action of urocortin in postconditioning involves recovery of intracellular
669 calcium handling. *Cell Calcium* 50, 84–90.
- 670 13. Calderón-Sánchez, E., Díaz, I., Ordóñez, A., and Smani, T. (2016).
671 Urocortin-1 Mediated Cardioprotection Involves XIAP and CD40-Ligand
672 Recovery: Role of EPAC2 and ERK1/2. *PLoS One* 11, e0147375.
- 673 14. Díaz, I., Calderón-Sánchez, E., Toro, R. Del, Ávila-Médina, J., de Rojas-de
674 Pedro, E.S., Domínguez-Rodríguez, A., Rosado, J.A., Hmadcha, A.,
675 Ordóñez, A., and Smani, T. (2017). miR-125a, miR-139 and miR-324
676 contribute to Urocortin protection against myocardial ischemia-
677 reperfusion injury. *Sci. Rep.* 7, 8898.
- 678 15. Smani, T., Mayoral-Gonzalez, I., Galeano-Otero, I., Gallardo-Castillo, I.,
679 Rosado, J.A., Ordoñez, A., and Hmadcha, A. (2020). Non-coding RNAs
680 and Ischemic Cardiovascular Diseases. *Adv. Exp. Med. Biol.* 1229, 259–
681 271.
- 682 16. Nabeebaccus, A., Zheng, S., and Shah, A.M. (2016). Heart failure-potential
683 new targets for therapy. *Br. Med. Bull.* 119, 99–110.
- 684 17. Lucas, T., Bonauer, A., and Dimmeler, S. (2018). RNA Therapeutics in
685 Cardiovascular Disease. *Circ. Res.* 123, 205–220.
- 686 18. Galeano-Otero, I., Del Toro, R., Guisado, A., Díaz, I., Mayoral-González,
687 I., Guerrero-Márquez, F., Gutiérrez-Carretero, E., Casquero-Domínguez,

- 688 S., Díaz-de la Llera, L., Barón-Esquivias, G., et al. (2020). Circulating miR-
689 320a as a Predictive Biomarker for Left Ventricular Remodelling in STEMI
690 Patients Undergoing Primary Percutaneous Coronary Intervention. *J.*
691 *Clin. Med.* 9, 1051.
- 692 19. Fasanaro, P., D'Alessandra, Y., Di Stefano, V., Melchionna, R., Romani, S.,
693 Pompilio, G., Capogrossi, M.C., and Martelli, F. (2008). MicroRNA-210
694 modulates endothelial cell response to hypoxia and inhibits the receptor
695 tyrosine kinase ligand Ephrin-A3. *J. Biol. Chem.* 283, 15878–83.
- 696 20. Yano, Y., Ozono, R., Oishi, Y., Kambe, M., Yoshizumi, M., Ishida, T.,
697 Omura, S., Oshima, T., and Igarashi, K. (2006). Genetic ablation of the
698 transcription repressor Bach1 leads to myocardial protection against
699 ischemia/reperfusion in mice. *Genes to Cells* 11, 791–803.
- 700 21. Basaiyye, S.S., Naoghare, P.K., Kanojiya, S., Bafana, A., Arrigo, P.,
701 Krishnamurthi, K., and Sivanesan, S. (2018). Molecular mechanism of
702 apoptosis induction in Jurkat E6-1 cells by *Tribulus terrestris* alkaloids
703 extract. *J. Tradit. Complement. Med.* 8, 410–419.
- 704 22. Gao, Z., Gao, Q., and Lv, X. (2020). MicroRNA-668-3p Protects Against
705 Oxygen-Glucose Deprivation in a Rat H9c2 Cardiomyocyte Model of
706 Ischemia-Reperfusion Injury by Targeting the Stromal Cell-Derived
707 Factor-1 (SDF-1)/CXCR4 Signaling Pathway. *Med. Sci. Monit.* 26, e919601.
- 708 23. Rivier, J., Gulyas, J., Kirby, D., Low, W., Perrin, M.H., Kunitake, K.,
709 DiGrucchio, M., Vaughan, J., Reubi, J.C., Waser, B., et al. (2002). Potent and

- 710 long-acting corticotropin releasing factor (CRF) receptor 2 selective
711 peptide competitive antagonists. *J. Med. Chem.* 45, 4737–4747.
- 712 24. Rehmann, H. (2013). Epac-inhibitors: Facts and artefacts. *Sci. Rep.* 3, 1–6.
- 713 25. Heusch, G. (2020). Myocardial ischaemia–reperfusion injury and
714 cardioprotection in perspective. *Nat. Rev. Cardiol.* 17.
- 715 26. Keiper, M., Stope, M.B., Szatkowski, D., Böhm, A., Tysack, K., Vom Dorp,
716 F., Saur, O., Oude Weernink, P.A., Evellin, S., Jakobs, K.H., et al. (2004).
717 Epac- and Ca²⁺-controlled activation of Ras and extracellular signal-
718 regulated kinases by Gs-coupled receptors. *J. Biol. Chem.* 279, 46497–
719 46508.
- 720 27. Wright, S.P., Doughty, R.N., Frampton, C.M., Gamble, G.D., Yandle, T.G.,
721 and Richards, A.M. (2009). Plasma urocortin 1 in human heart failure.
722 *Circ. Hear. Fail.* 2, 465–471.
- 723 28. Smani, T., Calderón-Sanchez, E., Gómez-Hurtado, N., Fernández-Velasco,
724 M., Cachafeiro, V., Lahera, V., Ordoñez, A., and Delgado, C. (2010).
725 Mechanisms underlying the activation of L-type calcium channels by
726 urocortin in rat ventricular myocytes. *Cardiovasc. Res.* 87, 459–466.
- 727 29. Tang, W.H.W., Shrestha, K., Martin, M.G., Borowski, A.G., Jasper, S.,
728 Yandle, T.G., Richards, A.M., Klein, A.L., and Troughton, R.W. (2010).
729 Clinical significance of endogenous vasoactive neurohormones in chronic
730 systolic heart failure. *J. Card. Fail.* 16, 635–640.
- 731 30. Giamouridis, D., Gao, M.H., Lai, N.C., Guo, T., Miyanohara, A.,

- 732 Blankesteyjn, W.M., Biessen, E.A.L., and Hammond, H.K. (2020).
733 Urocortin 2 Gene Transfer Improves Heart Function in Aged Mice. *Mol.*
734 *Ther.* 28, 180–188.
- 735 31. Giamouridis, D., Gao, M.H., Lai, N.C., Tan, Z., Kim, Y.C., Guo, T.,
736 Miyanochara, A., Blankesteyjn, W.M., Biessen, E., and Hammond, H.K.
737 (2018). Effects of Urocortin 2 Versus Urocortin 3 Gene Transfer on Left
738 Ventricular Function and Glucose Disposal. *JACC Basic to Transl. Sci.* 3,
739 249–264.
- 740 32. Zhou, Y., Chen, Q., Lew, K.S., Richards, A.M., and Wang, P. (2016).
741 Discovery of Potential Therapeutic miRNA Targets in Cardiac Ischemia-
742 Reperfusion Injury. *J. Cardiovasc. Pharmacol. Ther.* 21, 296–309.
- 743 33. Xiao, L., He, H., Ma, L., Da, M., Cheng, S., Duan, Y., Wang, Q., Wu, H.,
744 Song, X., Duan, W., et al. (2017). Effects of miR-29a and miR-101a
745 Expression on Myocardial Interstitial Collagen Generation After Aerobic
746 Exercise in Myocardial-infarcted Rats. *Arch. Med. Res.* 48, 27–34.
- 747 34. Qin, R.H., Tao, H., Ni, S.H., Shi, P., Dai, C., and Shi, K.H. (2018).
748 microRNA-29a inhibits cardiac fibrosis in Sprague-Dawley rats by
749 downregulating the expression of DNMT3A. *Anatol. J. Cardiol.* 20, 198–
750 205.
- 751 35. Jing, X., Yang, J., Jiang, L., Chen, J., and Wang, H. (2018). MicroRNA-29b
752 Regulates the Mitochondria-Dependent Apoptotic Pathway by Targeting
753 Bax in Doxorubicin Cardiotoxicity. *Cell. Physiol. Biochem.* 48, 692–704.

- 754 36. Shakeri, R., Kheirollahi, A., and Davoodi, J. (2017). Apaf-1: Regulation
755 and function in cell death. *Biochimie* 135, 111–125.
- 756 37. Wang, Y., Zhang, Q., Zhong, L., Lin, M., Luo, X., Liu, S., Xu, P., Liu, X.,
757 and Zhu, Y.Z. (2017). Apoptotic Protease Activating Factor-1 Inhibitor
758 Mitigates Myocardial Ischemia Injury via Disturbing Procaspace-9
759 Recruitment by Apaf-1. *Oxid. Med. Cell. Longev.* 2017.
- 760 38. Sanchis, D., Mayorga, M., Ballester, M., and Comella, J.X. (2003). Lack of
761 Apaf-1 expression confers resistance to cytochrome c-driven apoptosis in
762 cardiomyocytes. *Cell Death Differ.* 10, 977–986.
- 763 39. Bilbija, D., Gravning, J.A., Haugen, F., Attramadal, H., and Valen, G.
764 (2012). Protecting the heart through delivering DNA encoding for heme
765 oxygenase-1 into skeletal muscle. *Life Sci.* 91, 828–836.
- 766 40. Preda, M.B., Rønningen, T., Burlacu, A., Simionescu, M., Moskaug, J.Ø.,
767 and Valen, G. (2014). Remote Transplantation of Mesenchymal Stem Cells
768 Protects the Heart Against Ischemia-Reperfusion Injury. *Stem Cells* 32,
769 2123–2134.
- 770 41. Czibik, G., Gravning, J., Martinov, V., Ishaq, B., Knudsen, E., Attramadal,
771 H., and Valen, G. (2011). Gene therapy with hypoxia-inducible factor 1
772 alpha in skeletal muscle is cardioprotective in vivo. *Life Sci.* 88, 543–550.
- 773 42. Depre, C., and Taegtmeyer, H. (2000). Metabolic aspects of programmed
774 cell survival and cell death in the heart. *Cardiovasc. Res.* 45, 538–548.
- 775 43. Zhang, S., Yin, Z., Dai, F., Wang, H., Zhou, M., Yang, M., Zhang, S., Fu,

- 776 Z., Mei, Y., Zang, M., et al. (2019). miR-29a attenuates cardiac
777 hypertrophy through inhibition of PPAR δ expression. *J. Cell. Physiol.* *234*,
778 13252–13262.
- 779 44. Caravia, X.M., Fanjul, V., Oliver, E., Roiz-Valle, D., Morán-Álvarez, A.,
780 Desdín-Micó, G., Mittelbrunn, M., Cabo, R., Vega, J.A., Rodríguez, F., et
781 al. (2018). The microRNA-29/PGC1 α regulatory axis is critical for
782 metabolic control of cardiac function. *PLoS Biol.* *16*, e2006247.
- 783 45. Tomczyk, M., Kraszewska, I., Dulak, J., and Jazwa-Kusior, A. (2019).
784 Modulation of the monocyte/macrophage system in heart failure by
785 targeting heme oxygenase-1. *Vascul. Pharmacol.* *112*, 79–90.
- 786 46. van Rooij, E., Sutherland, L.B., Thatcher, J.E., DiMaio, J.M., Naseem, R.H.,
787 Marshall, W.S., Hill, J.A., and Olson, E.N. (2008). Dysregulation of
788 microRNAs after myocardial infarction reveals a role of miR-29 in cardiac
789 fibrosis. *Proc. Natl. Acad. Sci.* *105*, 13027–13032.
- 790 47. Calderon-Sanchez, E., Diaz, I., Ordonez, A., and Smani, T. (2016).
791 Urocortin-1 Mediated Cardioprotection Involves XIAP and CD40-Ligand
792 Recovery: Role of EPAC2 and ERK1/2. *PLoS One* *11*.
793
794

795 **TABLE**

796

797 **TABLE 1.** Data summary (mean \pm SEM) of hemodynamic parameters evaluated in rats 1 week
 798 after surgery in the following experimental group: Sham, "I/R", and "I/R + Ucn-2". LVdD is for
 799 left ventricle diastolic diameter; LVEF: left ventricle ejection fraction; LVEdV: left ventricle end-
 800 diastolic volume; LVFS: left ventricle fractional shortening; LVEsV: left ventricle end-systolic
 801 volume. "***" and "#" indicate significance at $p < 0.05$ in Sham vs I/R and I/R vs IR+Ucn2,
 802 respectively.

803

	LVEdV (ml)	LVEsV (ml)	LVdD (mm)	LVEF (%)	LVFS (%)
Sham (n=10)	0.42 \pm 0.02	0.12 \pm 0.01	5.91 \pm 0.18	71.84 \pm 1.23	19.98 \pm 1.90
I/R (n=12)	0.50 \pm 0.03*	0.20 \pm 0.02*	6.85 \pm 0.27*	60.16 \pm 2.04*	16.77 \pm 1.1*
I/R + Ucn-2 (n=15)	0.40 \pm 0.02#	0.13 \pm 0.01#	6.46 \pm 0.16	66.43 \pm 0.68*#	18.16 \pm 3.20

804

805

806

807 **FIGURE LEGENDS**

808

809 **FIGURE 1. I/R increases of circulating urocortin-2 level and the expression of**

810 **CRF-R2.** (A) Bar graph shows the concentration of circulating Ucn-2 in serum of
 811 rats from sham, I/R 1 week (I/R 1w) and 6 weeks (I/R 6w) after surgery (n = 7-11).

812 (B) Plot of western blot and bar graph summarizing the expression of CRF-R2
 813 expression and tubulin in rats' heart from sham, I/R (1 and 6 weeks) after surgery
 814 (n = 8). Values are means \pm SEM. "***" and "****" indicate significance at $p < 0.01$
 815 and $p < 0.001$, respectively.

816 **FIGURE 2. Urocortin-2 improves contractility and prevents I/R-induced**

817 **fibrosis.** (A) Representative M-mode echocardiographic images evaluated 1

818 week after the intervention in Sham, I/R rats, and in rats infused with 150 μ g/Kg

819 Ucn-2 (I/R + Ucn2). (B) Representative *in vivo* cardiac magnetic resonance images
820 taken from I/R and I/R + Ucn-2 rats. Gadolinium was used as contrast. The fibrotic
821 area is delimited by yellow lines. (C) Bar graph showing summary data of fibrotic
822 areas in I/R and I/R + Ucn-2 rats. (D) Panel shows representative Masson's
823 trichrome staining of transverse heart sections from I/R and I/R + Ucn-2. Healthy
824 tissue is stained by red, while fibrotic tissue in the infarcted zone is stained in
825 blue. (E-H) Bar graphs show the effect of Ucn-2 on the expression of pro-fibrotic
826 genes, collagen I (*Col-I*, E), collagen III (*Col-III*, F), Transforming growth factor $\beta 1$
827 (*Tgf- $\beta 1$* , G), and *Tgf- $\beta 2$* (H), examined in the risk zone of the infarcted hearts 1
828 week after surgeries. Samples were from "Sham"; I/R and I/R + Ucn-2. Gene's
829 relative expression was calculated using the $2^{-\Delta\Delta C_t}$ method after normalization to
830 the internal control β -actin. Data are relative expression of Log fold change of
831 means \pm SEM (n = 4-8). "**", "***", "****" and "*****" indicate significance at $p < 0.05$,
832 $p < 0.01$, $p < 0.001$ and $p < 0.0001$, respectively.

833 **FIGURE 3. Urocortin-2 attenuates the release of LDH and apoptosis.** (A) Bar
834 graph shows the level of LDH in the serum of rats from Sham, I/R and I/R + Ucn-
835 2, 24 h after surgery. (B) Representative snapshot of Tunnel staining (green) in
836 adult heart section from rats of the three experimental groups. Top: images taken
837 with a 10X objective, scale bar = 1 mm. Bottom: images cropped from upper ones.
838 (C) Representative images of heart sections stained for detection of cleaved
839 caspase 3 (upper panel) captured with a 40X objective, scale bar = 100 μ m. Lower
840 panel shows merge images of heart's section stained with caspase 3 in red, wheat

841 germ agglutinin (WGA) in green and DAPI in blue used for nuclear staining. (D)
842 Representative images of annexin V (green) staining in adult cardiac myocytes
843 cells. Images are from untreated cells (control), and from cells exposed to I/R (30
844 min/24 h each) \pm Ucn-2 (30 nM). Image were taken with a 20X objective, scale bar
845 = 100 μ m. (E, F) Summary data showing the percentage of unstained live cardiac
846 myocytes, and annexin V-labeled cells related to control. Values are means \pm SEM
847 (n = 4-6). “*”, “***”, and “****” indicate significance at $p < 0.05$, $p < 0.01$ and $p < 0.001$,
848 respectively.

849 **FIGURE 4. miRNAs expression in serum and heart tissue of STEMI patients,**
850 **and in rat cardiac ventricle risk zone.** (A) Bar graph summarizing microarray
851 results indicating release of circulating miRNAs examined in the serum of STEMI
852 patients 3-6 h after primary percutaneous coronary intervention. (B) Bar graph
853 shows the detection of selected miRNAs in the atrium of ischemic patients with
854 heart failure. Δ Ct represents the level of Ct of miRNAs compared to the
855 endogenous control. Values are means \pm SEM (n = 8-10). (C-H) Bar graphs show
856 the expression of miR-29a (C), miR-103 (D), miR-133 (E), miR-339-5p (F), miR-
857 423_1 (G) and miR-451_1* (H) examined in the risk zone of the infarcted heart of
858 sham, I/R and I/R+Ucn-2, 24 h and 1 week after surgery. Relative expression
859 levels were calculated using the $2^{-\Delta\Delta Ct}$ method after normalization to the
860 expression of the endogenous control miRTC1. Values are relative expression of
861 Log fold change of means \pm SEM (n = 4-6). “*”, “***”, “****” and “*****” indicate
862 significance at $p < 0.05$, $p < 0.01$, $p < 0.001$ and $p < 0.0001$, respectively.

863 **FIGURE 5. miR-29a and miR-451_1* are predicted to target apoptosis-related**
864 **genes.** (A) PANTHER analysis showing the predicted pathways go be targeted
865 by miR-29a, miR-103, miR-133, miR-339-5p, miR-423_1 and miR-451_1*. The pink
866 and grey slice in the pie chart highlight predicted genes related to apoptosis and
867 fibrosis. (B) Number of predicted target genes for each miRNA. (C-E) Graphs
868 show of the expression of 76 dysregulated genes examined using samples (n = 4)
869 from NRVM exposed to I/R (C), and from NRVM transfected with mimics of
870 miR-29a (D) and miR-451_1* (E) in I/R. Inserts show numbers and percentage of
871 upregulated and downregulated genes in each condition.

872 **FIGURE 6. miR-29a regulates apoptotic and fibrotic genes under I/R, and**
873 **signaling pathway of miR-29a regulation by Ucn-2.** (A-F) Bar graphs showing
874 the expression of *Apaf-1*, *Aifm-1*, *Bcl-2*, *Cyts*, *Hmox-1* and *Mapk-8*, in control, in
875 non-transfected NVRM under I/R (orange), and in NRVM transfected with miR-
876 29a (red) and 451_1* (green). (G, H) Bar graphs showing the expression of *Col- I*
877 and *Col-III* in similar conditions as in above. (I) Bar graph shows the expression
878 of miR-29a examined in untreated NRVM "Control", in NRVM under "I/R", in
879 NRVM treated with Ucn-2 (10 nM) before reperfusion "I/R + Ucn-2", and in
880 NRVM pretreated with Astressin (1 μ M) to inhibit CRF-R2 "I/R+Ucn-2+Ast", H89
881 (1 μ M) to inhibit PKA "I/R+Ucn-2+H89", ESI-05 (10 μ M) to block Epac2 "I/R+Ucn-
882 2+ESI", and PD 098059 (5 μ M) to inhibit ERK1/2 "I/R+Ucn-2+PD". Ucn-2 was
883 added before reperfusion. Relative expression levels were calculated using the
884 $2^{-\Delta\Delta Ct}$ method after normalization with the expression of the endogenous control

885 β -actin for genes and miRTC1 for miR-29a. Values are expressed as relative
886 expression of Log fold change of means \pm SEM (n = triplicate of 3-4 cell culture).
887 “*”, “***”, and “*****” indicate significance at $p < 0.05$, $p < 0.01$, and $p < 0.0001$,
888 respectively.

889 **FIGURE 7. Expression of apoptotic genes and protein I/R rat model.** (A-D) Bar
890 graphs showing the relative expressions of *Hmox-1*, *Aifm-1*, *Apaf-1*, and *Cyts*
891 calculated using the $2^{-\Delta\Delta Ct}$ method after normalization with the expression of the
892 endogenous control β -actin. (E-G) Representative immunoblots and summary
893 data of protein expression of HMOX-1, AIFM-1, and CYCS assessed by western
894 blots and normalized to their corresponding GAPDH expression. GAPDH blots
895 in 7F and 7G are the same. Samples were from sham, I/R, and I/R + Ucn-2 rats,
896 and were processed 24 h and 1 week after surgery. Values are from n = 3-4. “*”,
897 “***” and “*****” indicate significance at $p < 0.05$, $p < 0.01$ and $p < 0.001$ respectively.

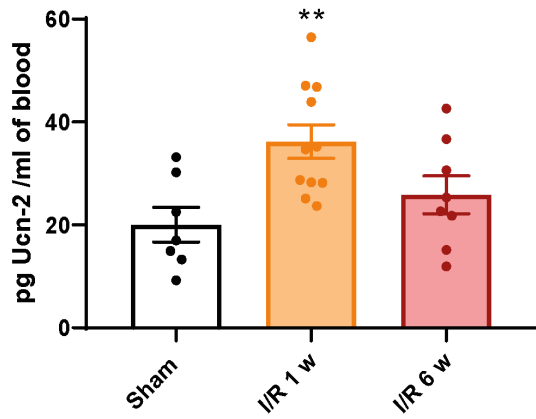
898 **FIGURE 8. Expression of apoptotic genes in left ventricles of ischemic patients**
899 **with heart failure.** (A) Bar graph showing the expression of *Hmox-1*, *Mapk-8*,
900 *Cyts*, *Apaf-1*, and *Aifm-1*, in ventricle biopsies from ischemic patients with heart
901 failure, as compared to a healthy ventricle. (B-F) Graphs showing linear
902 regression analysis using the percentage of the left ventricular ejection fraction
903 (LVEF) vs the expression of *Hmox-1*, *Mapk-8*, *Cyts*, *Apaf-1*, and *Aifm-1*. Relative
904 expression levels were calculated using the $2^{-\Delta\Delta Ct}$ method after normalization
905 with the expression of the endogenous control β -actin. Values are expressed as

906 relative expression of Log fold change of means \pm SEM (n = 7). “*”, “**” and “****”

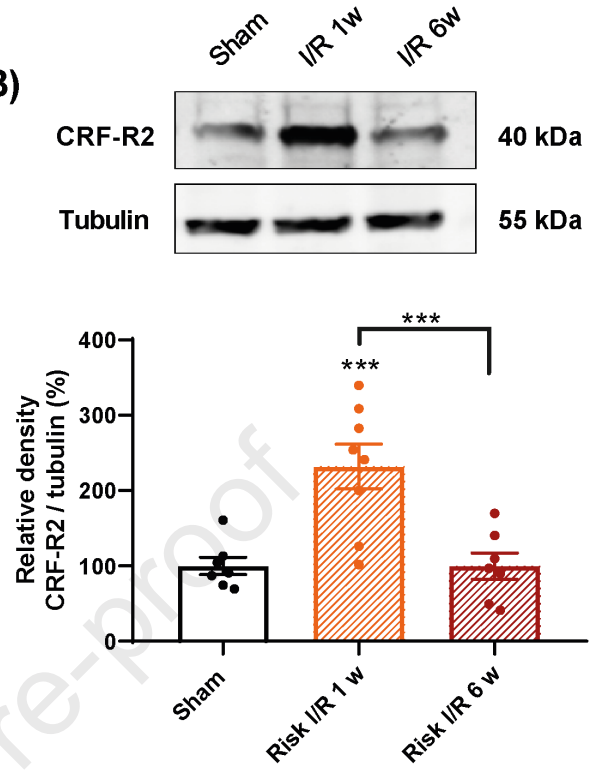
907 indicate significance at $p < 0.05$, $p < 0.01$ and $p < 0.0001$ respectively.

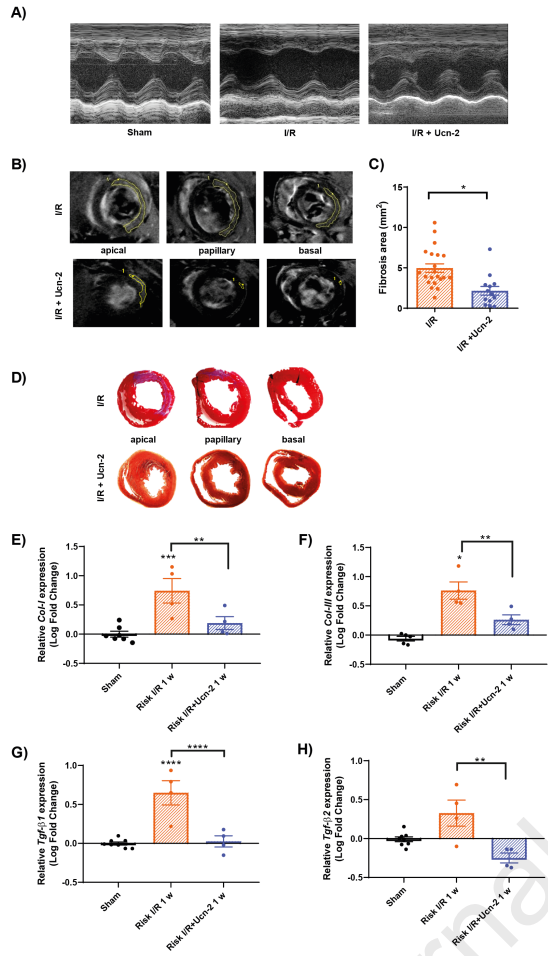
Journal Pre-proof

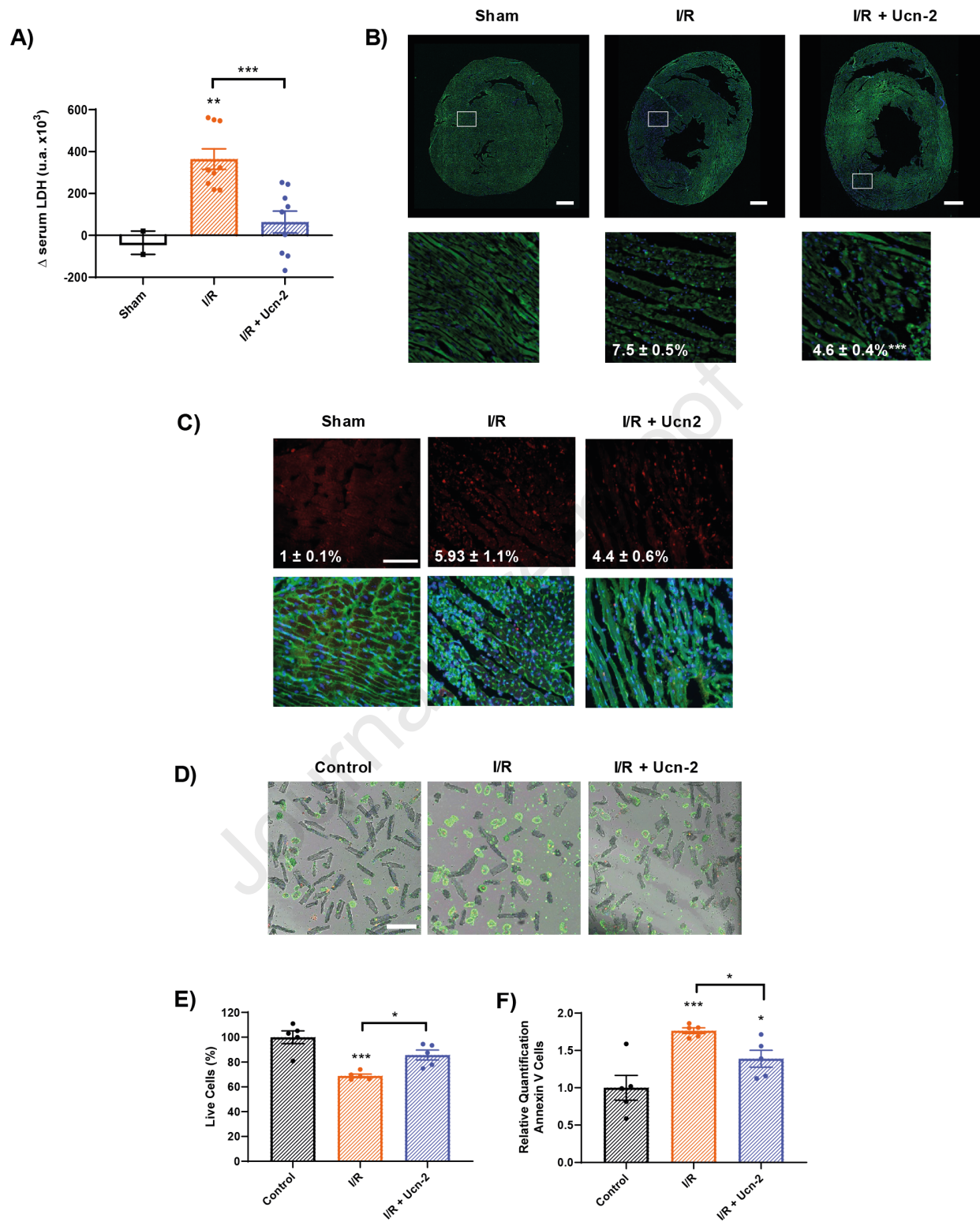
A)

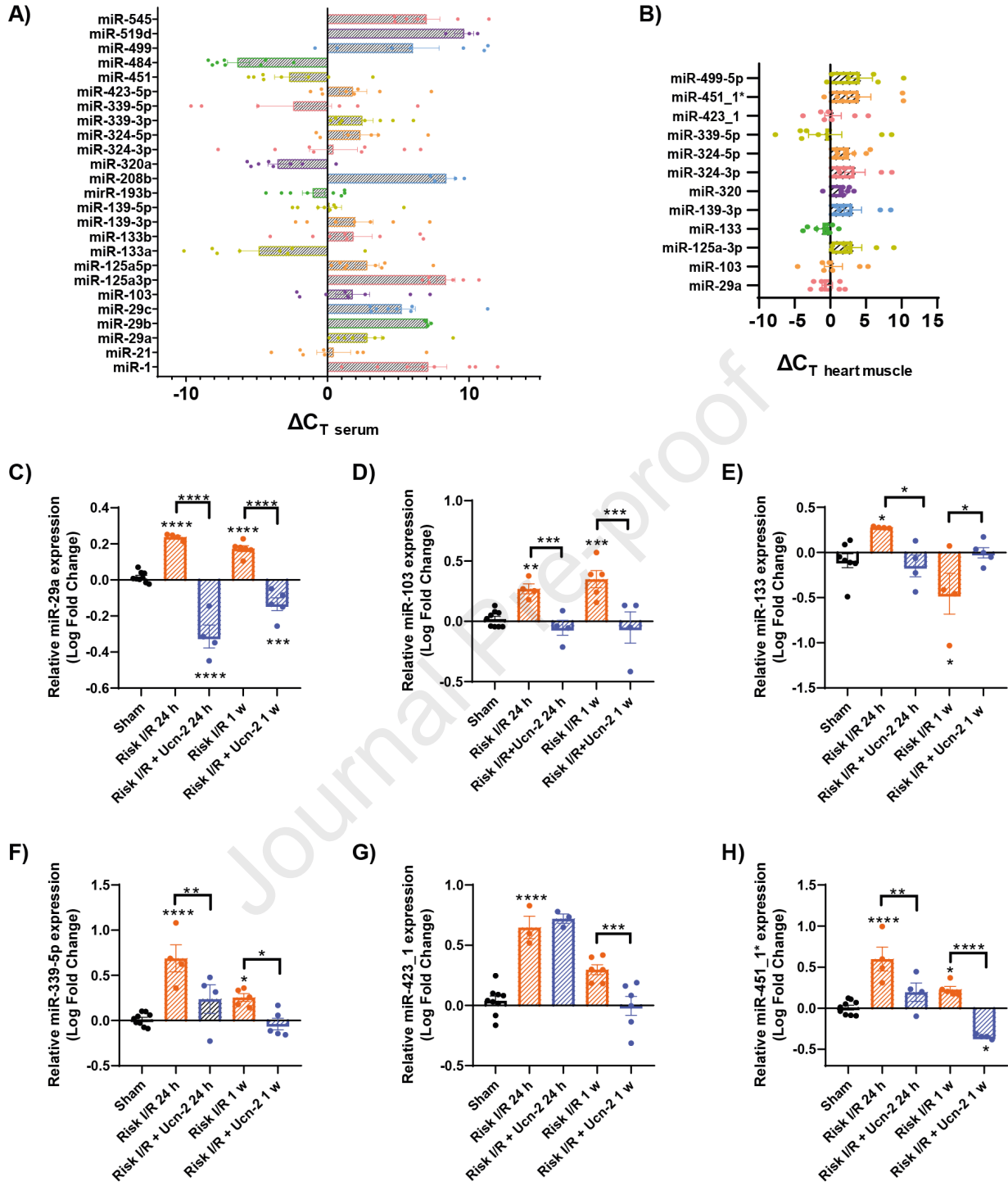


B)

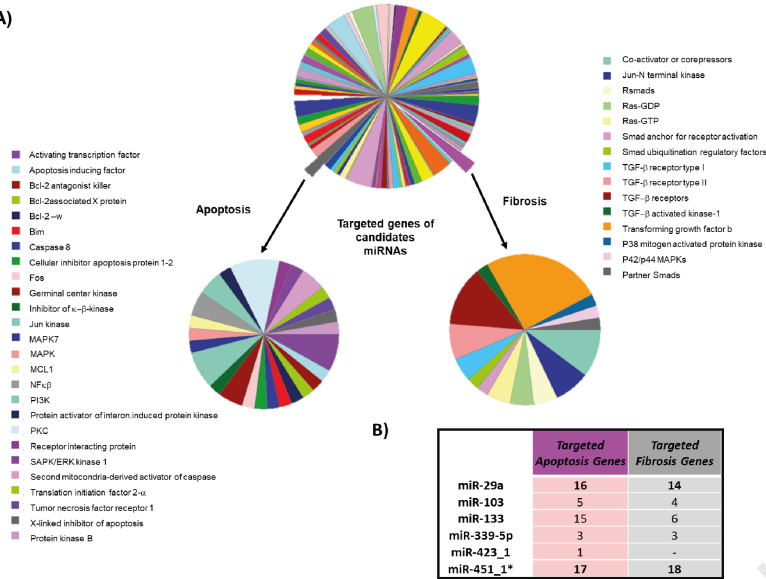








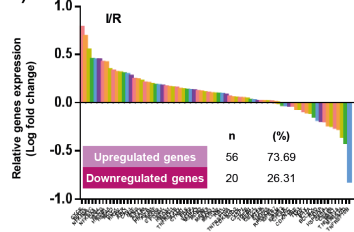
A)



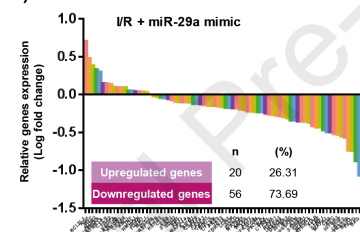
B)

	Targeted Apoptosis Genes	Targeted Fibrosis Genes
miR-29a	16	14
miR-103	5	4
miR-133	15	6
miR-339-5p	3	3
miR-423_1	1	-
miR-451_1*	17	18

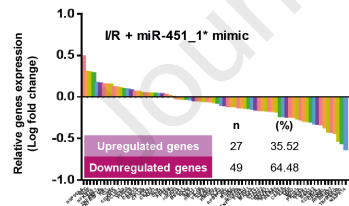
C)

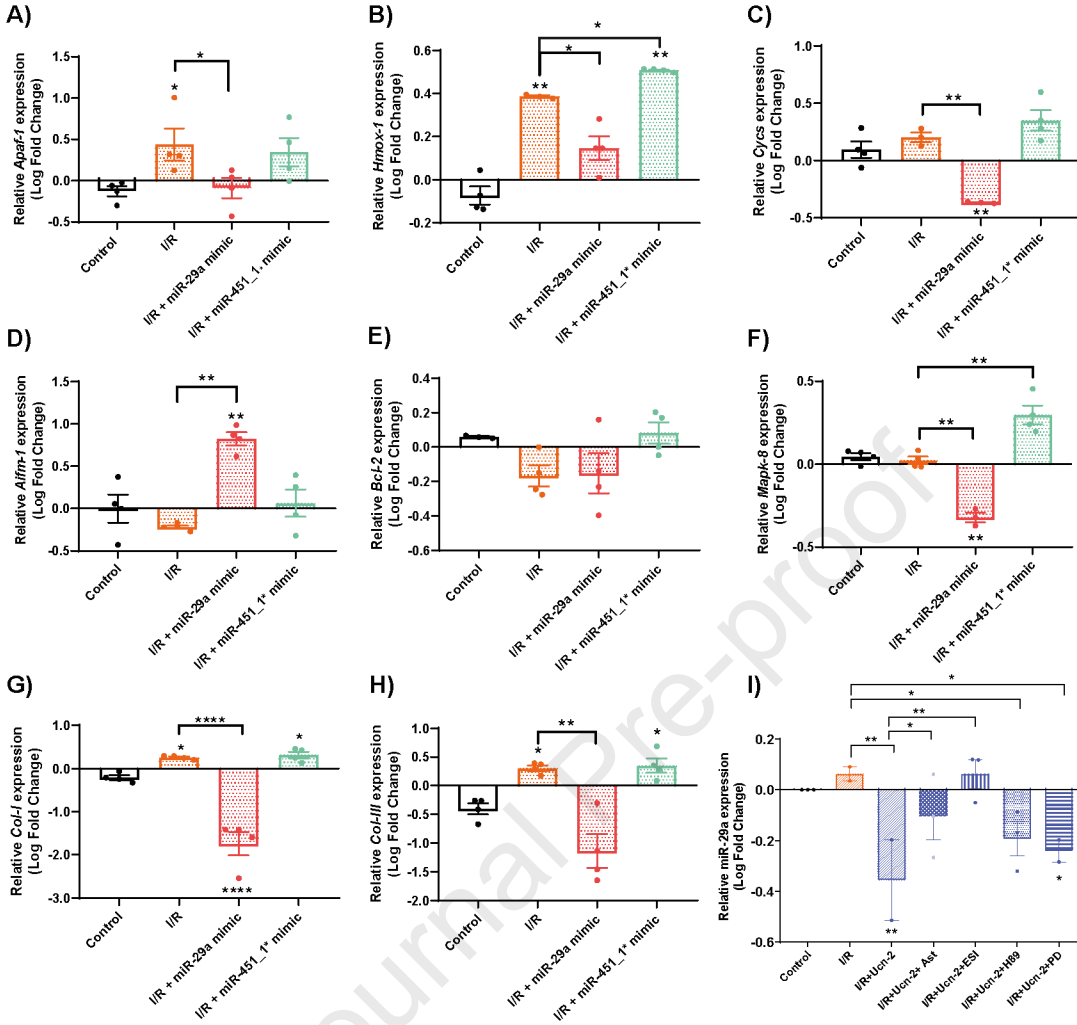


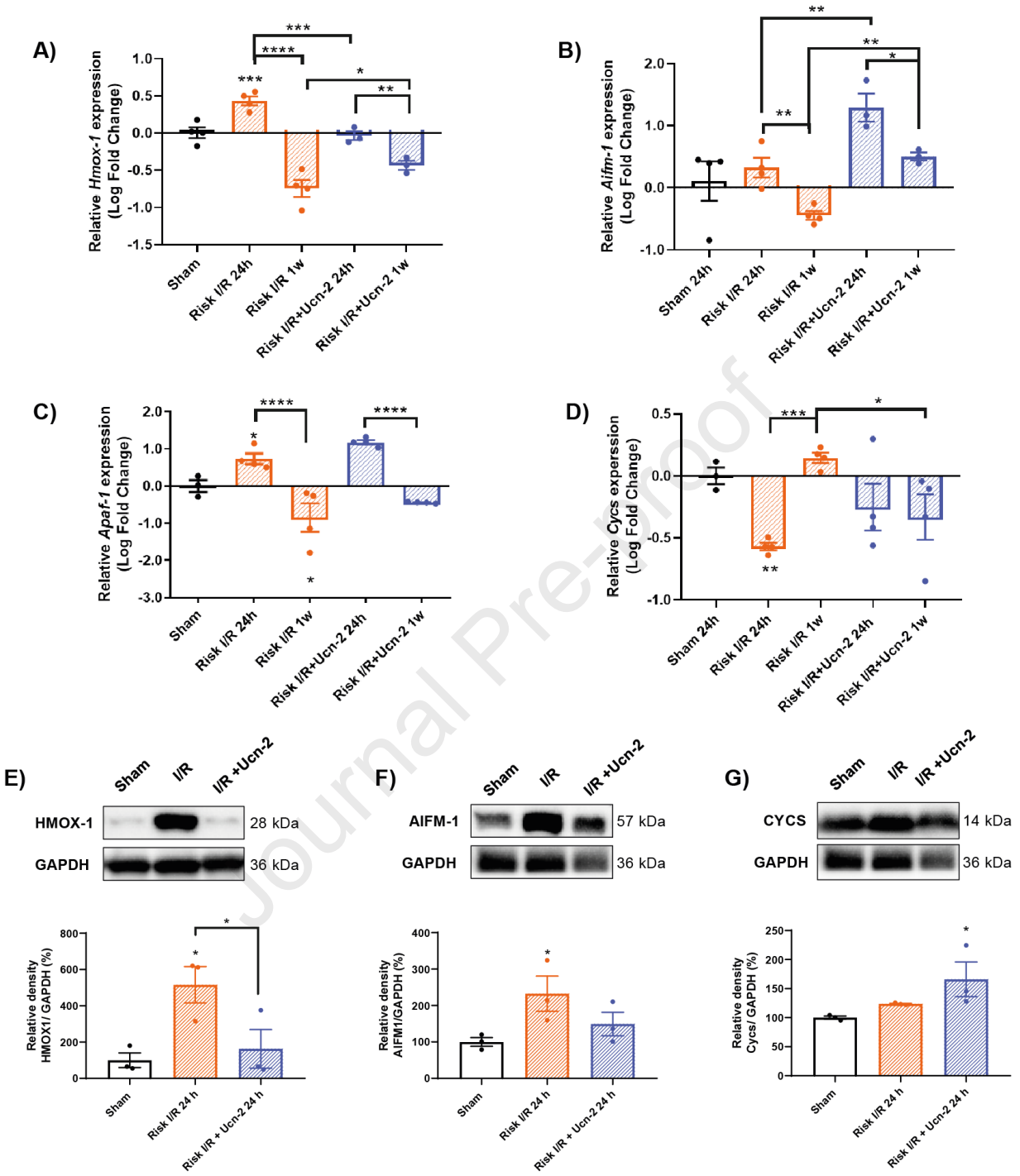
D)

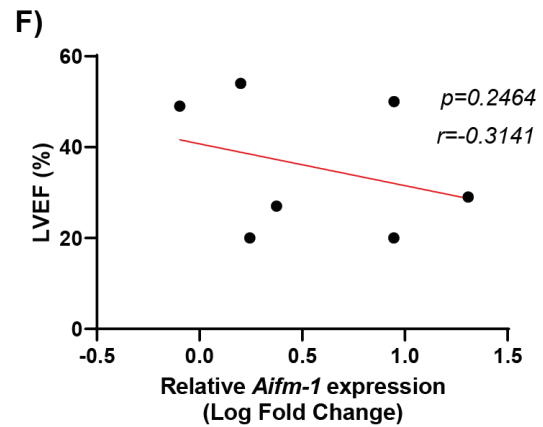
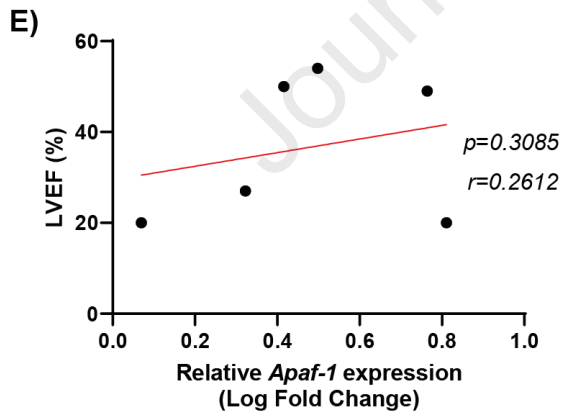
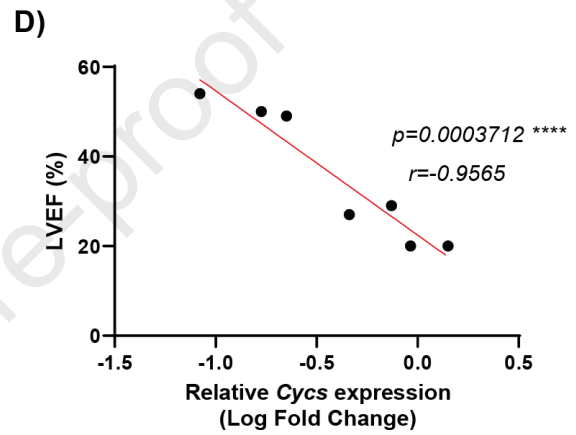
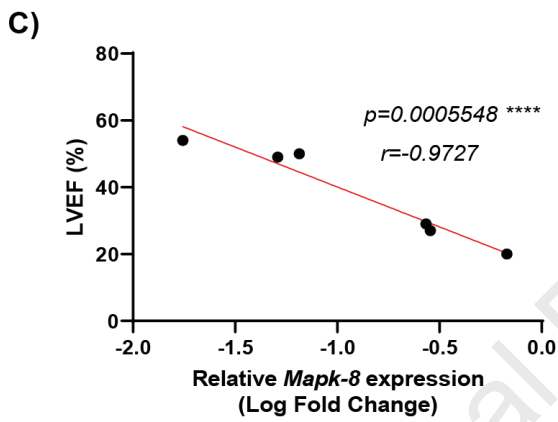
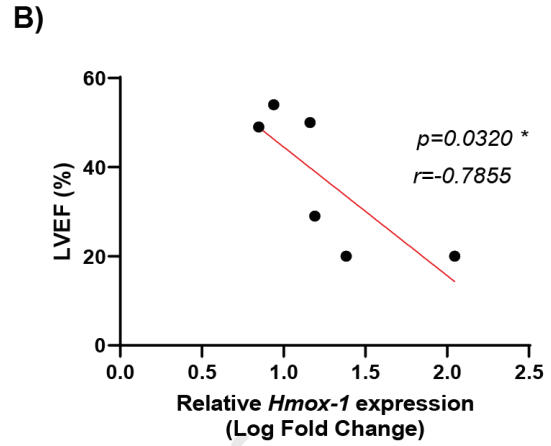
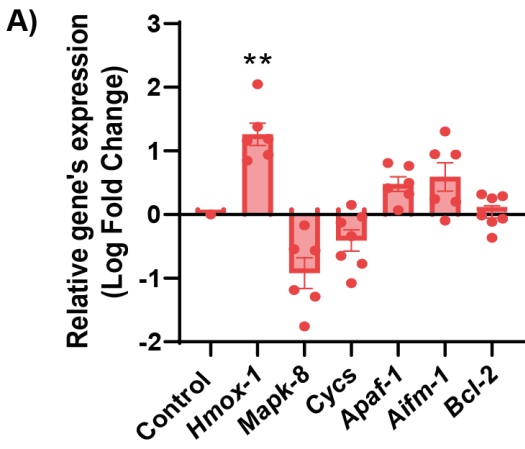


E)









eTOC Synopsis

Mayoral-González et al. used heart samples from ischemic patients and animal models to demonstrate the sustained protective role of Urocortin-2, which induced changes in the expression of miR-29a and specific genes associated with cardiomyocyte death and fibrosis, critical events in the progression of adverse cardiac remodelling towards heart failure.

Journal Pre-proof